# Bundle-like α`-$NaV_2O_5$ Mesocrystals: from Synthesis, Growth Mechanism to Analysis of Na-ion Intercalation/Deintercalation Abilities

Pengcheng Liu[1,4], Dehua Zhou[2], Kongjun Zhu[1]*, Qingliu Wu[3]*, Yifeng Wang[5], Guoan Tai[1], Wei Zhang[1,4], Qilin Gu[1,4]

[1]State Key Laboratory of Mechanics and Control of Mechanical Structures, Nanjing University of Aeronautics and Astronautics, Nanjing 210016, China

[2]Department of Chemical Engineering, University of Rochester, Rochester, New York 14627, USA

[3]Chemical and Materials Engineering Department, University of Kentucky, 177 F. P. Anderson Tower, Lexington, KY, 40506-0046, USA

[4]College of Materials Science and Technology, Nanjing University of Aeronautics and Astronautics, 210016, China

[5]College of Materials Science and Engineering, Nanjing Tech University, Nanjing, 210009, China

*Corresponding author

Kongjun Zhu: Tel: +86-25-84893466-190, Fax: +86-25-84895759,

E-mail: kjzhu@nuaa.edu.cn

Qingliu Wu: Tel: 01-859-327-2908

E-mail: qwu4@uky.edu

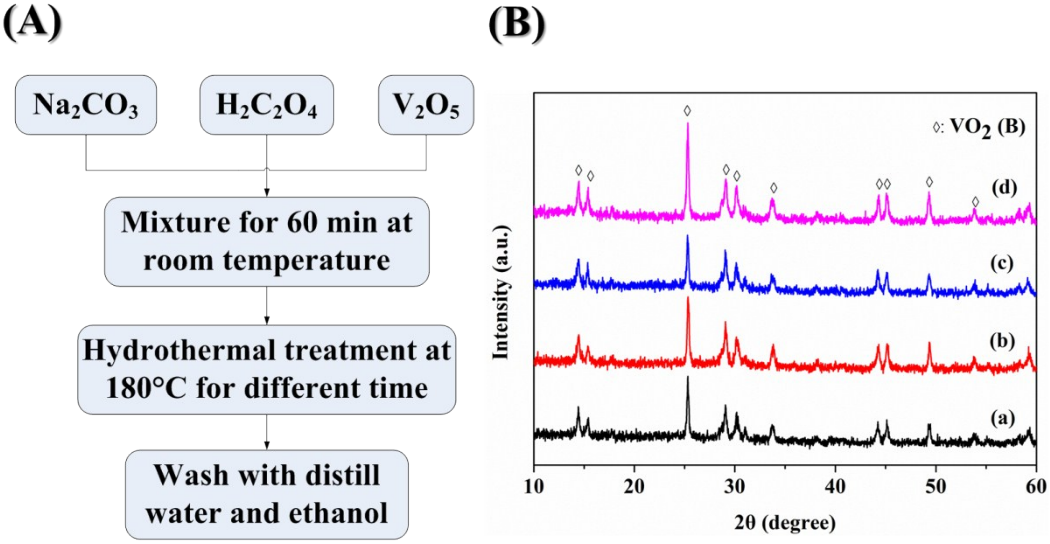

**Figure S1.** (A) Flow charts of initial one-step hydrothermal methods utilized for $NaV_2O_5$ preparation; (B) XRD patterns of samples obtained from initial one-step hydrothermal method. All samples were hydrothermally treated at 180 ºC for (a) 12 h; (b) 24 h; (c) 36 h; (d) 48 h..

## Discussion on XRD (Figure S1)

We attempted initially to prepare $NaV_2O_5$ by mixing $V_2O_5$, $Na_2CO_3$ and $H_2C_2O_4{\cdot}2H_2O$ together directly, and then above mixing solution was transferred into autoclave with heated to 180 °C for various time, as shown in Figure S1(A). However, instead of expected $NaV_2O_5$ product, merely $VO_2$ (B) was observed in the finally resulted products, even as the reaction time reached up to 48 h (Figure S1(B)). It is highly possible that the hydrolysis of $Na_2CO_3$ and $V_2O_5$ are slow processes, but the reduction reaction rate of $V_2O_5$ by the oxalic acid is greatly faster than the hydrolysis rate of $Na_2CO_3$.[1, 2] So that, $VO_2$ will be formed firstly through reducing reaction, but then, $Na^+$ ions will be hardly to be inserted into the reduced $VO_2$ product.[3, 4] Therefore, only $VO_2$ is observed in the finally resulted products.

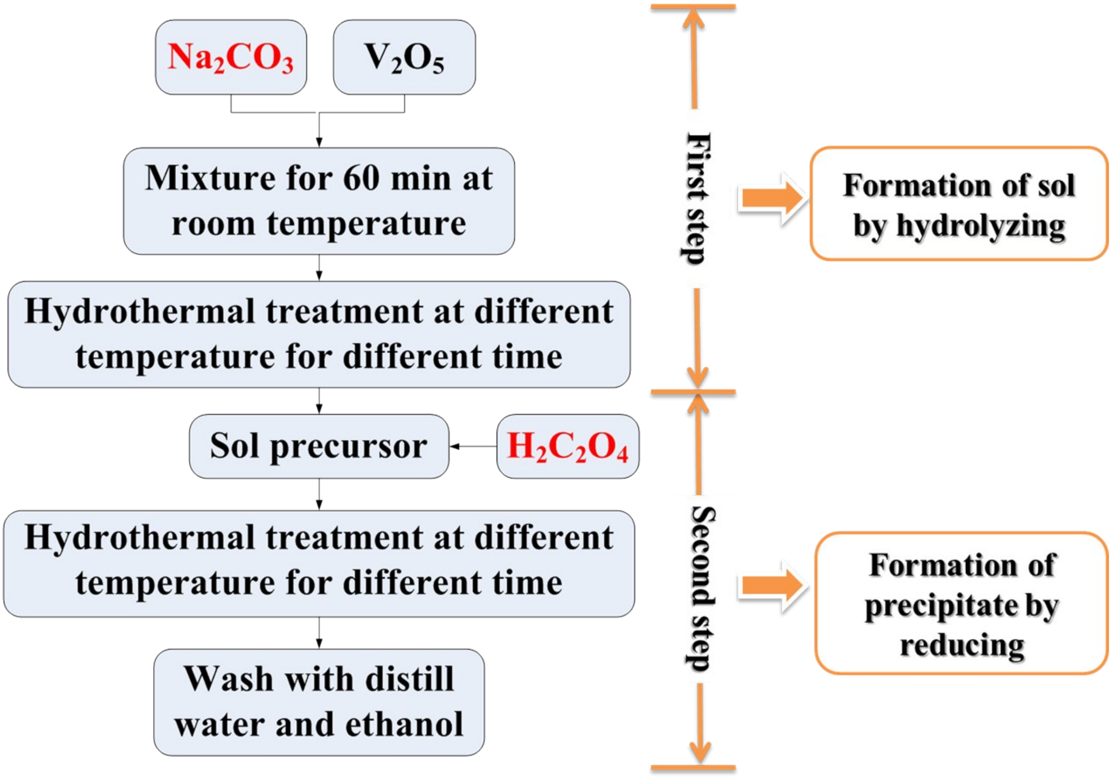

**Figure S2.** Flow charts of two-step hydrothermal methods utilized for $NaV_2O_5$ preparation.

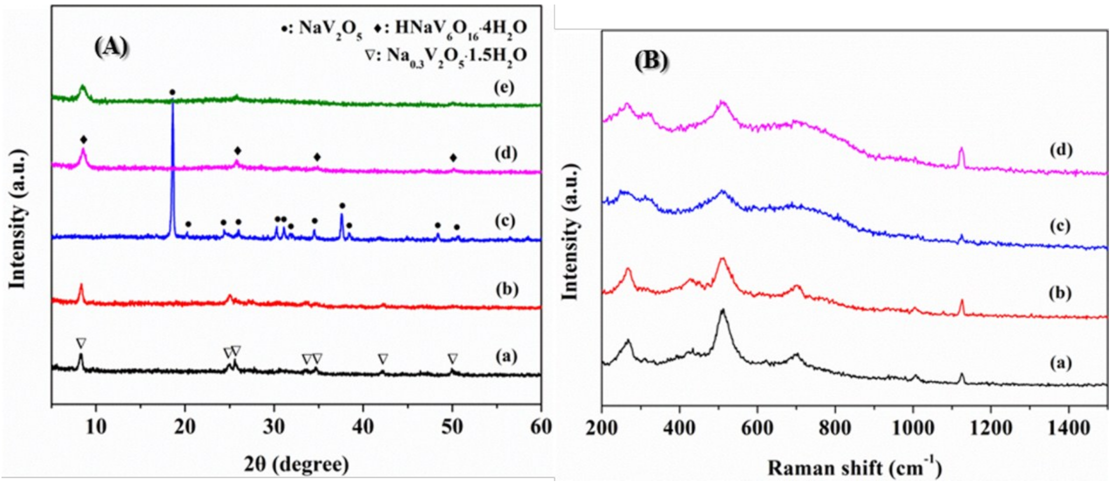

**Figure S3.** XRD patterns and Raman spectra of samples obtained at different temperature for the first step time of 48 h and the second one of 48 h under the two-step hydrothermal conditions. (A) XRD patterns: (a) 140 ºC, (b) 160 ºC, (c) 180 ºC, (d) 200 ºC, (e) 220 ºC; (B) Raman spectra: (a) 140 ºC, (b) 160 ºC, (c) 200 ºC, (d) 220 ºC.

## Discussion on XRD and Raman (Figure S3)

The analysis on the XRD measurements shows that $NaV_2O_5$ can be successfully synthesized at 180 °C, when both reaction time for the first and second step were fixed as 48 h (Figure S3A(c)). However, the final product was $Na_{0.3}V_2O_5{\cdot}1.5H_2O$ (exhibiting as green powders under the visual inspection) with the reaction temperature below 180 °C (Figures S3A(a) and (b)), while $HNaV_6O_{16}{\cdot}4H_2O$ (exhibiting as gray powders) obtained above 180 °C (Figures S3A(d) and (e)). The observations from XRD measurements are further confirmed by the phase analysis through Raman spectroscopy, shown in Figure S3B. The formation of final products through two-step hydrothermal approach is probably associated with the activity of ions, which is highly sensitive to the reaction temperature. Apparently, there exists an optimal temperature of 180 °C to synthesize $NaV_2O_5$ through the two-step hydrothermal approach with a certain reaction time.

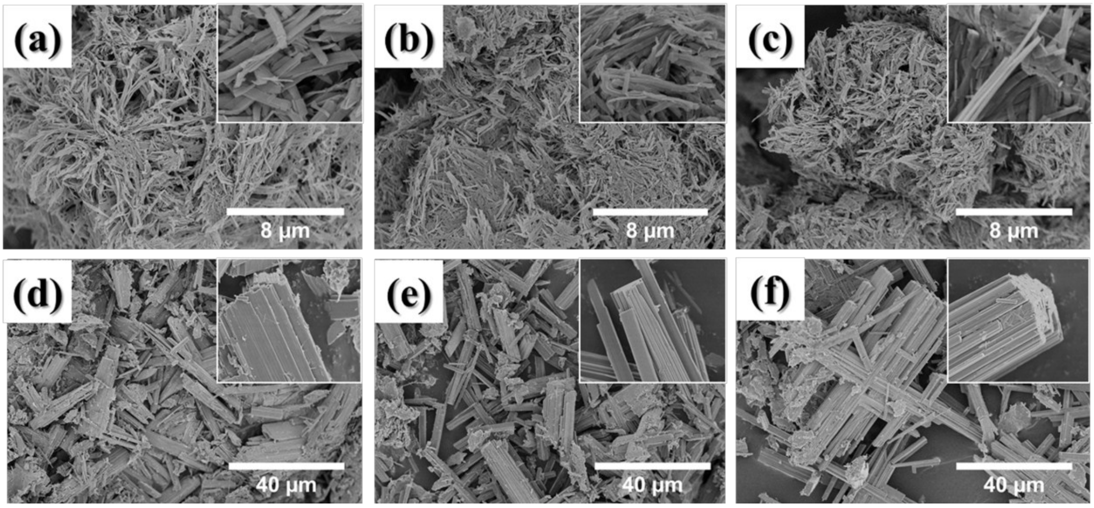

**Figure S4.** SEM images of samples prepared from two-step hydrothermal method. All samples were initially treated at 180 ºC for 48 hours, then further treated at 180 ºC for (a) 2 h, (b) 6 h, (c) 12 h, (d) 24 h, (e) 36 h, (f) 48 h during the second step.

## Discussion on SEM (Figure S4)

When the reaction time was 2 h, the feature of short nanobelt is observed on the final samples (Figure S4(a)), which is identified as $Na_{0.3}V_2O_5 \cdot 1.5H_2O$ from XRD (Figure 1B(a)). With the reaction time continuously increased, the feature of belts is observable on all samples, but the length of belts increases gradually (Figures S4(b) and (c)). When the reaction time reached to 24 h, bundle-like $NaV_2O_5$ mesocrystals are observed on the final products (Figure S4(d)). Similar to the first step, increasing the reaction time beyond 24 h only enhances the size of bunches composed of $NaV_2O_5$ belts (Figures S4(e) and (f)).

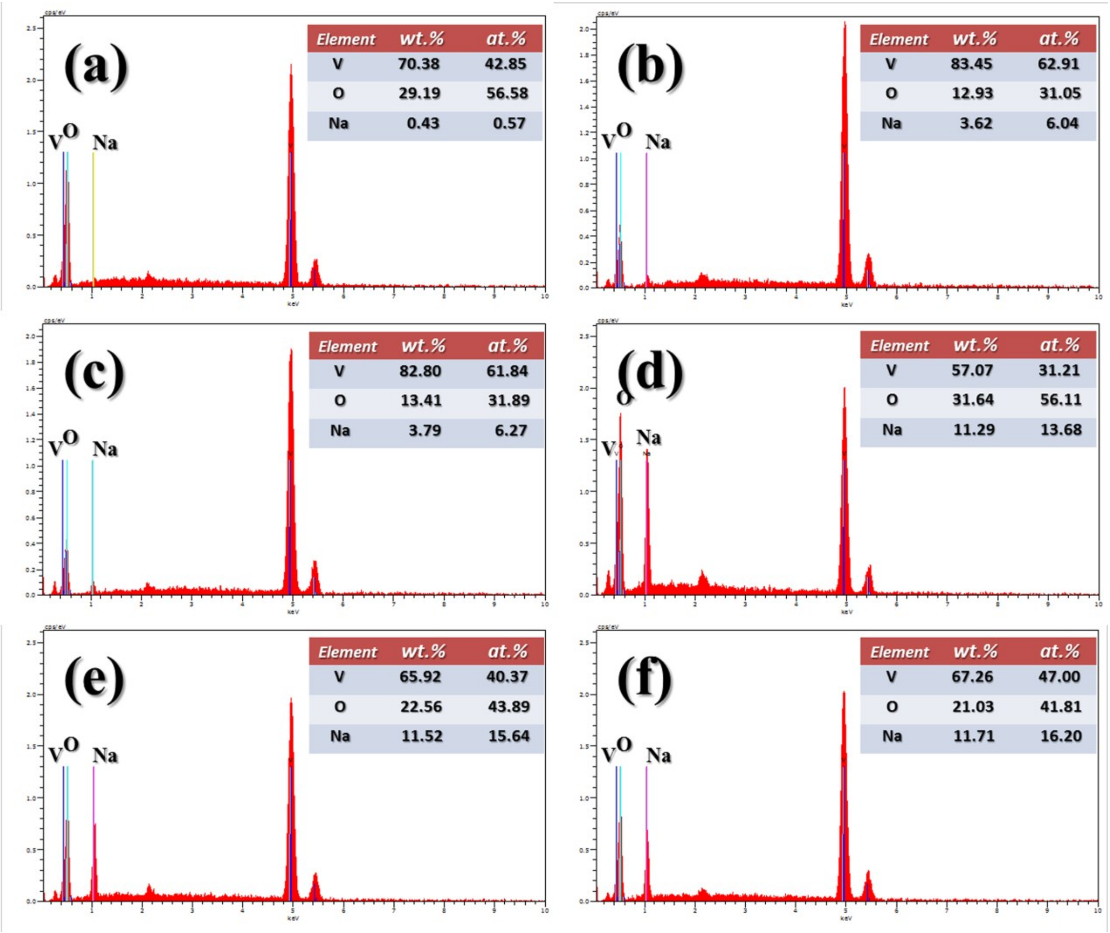

(a)

| Element | wt.% | at.% |
|---|---|---|
| V | 70.38 | 42.85 |
| O | 29.19 | 56.58 |
| Na | 0.43 | 0.57 |

(b)

| Element | wt.% | at.% |
|---|---|---|
| V | 83.45 | 62.91 |
| O | 12.93 | 31.05 |
| Na | 3.62 | 6.04 |

(c)

| Element | wt.% | at.% |
|---|---|---|
| V | 82.80 | 61.84 |
| O | 13.41 | 31.89 |
| Na | 3.79 | 6.27 |

(d)

| Element | wt.% | at.% |
|---|---|---|
| V | 57.07 | 31.21 |
| O | 31.64 | 56.11 |
| Na | 11.29 | 13.68 |

(e)

| Element | wt.% | at.% |
|---|---|---|
| V | 65.92 | 40.37 |
| O | 22.56 | 43.89 |
| Na | 11.52 | 15.64 |

(f)

| Element | wt.% | at.% |
|---|---|---|
| V | 67.26 | 47.00 |
| O | 21.03 | 41.81 |
| Na | 11.71 | 16.20 |

**Figure S5.** Energy spectrums of samples prepared from two-step hydrothermal method. All samples were initially treated in the first step at 180 °C for (a) 12 h, (b) 24 h, (c) 36 h, (d) 38 h, (e) 40 h, (f) 44 h, followed by treated at 180 °C for 48 hours in the second step.

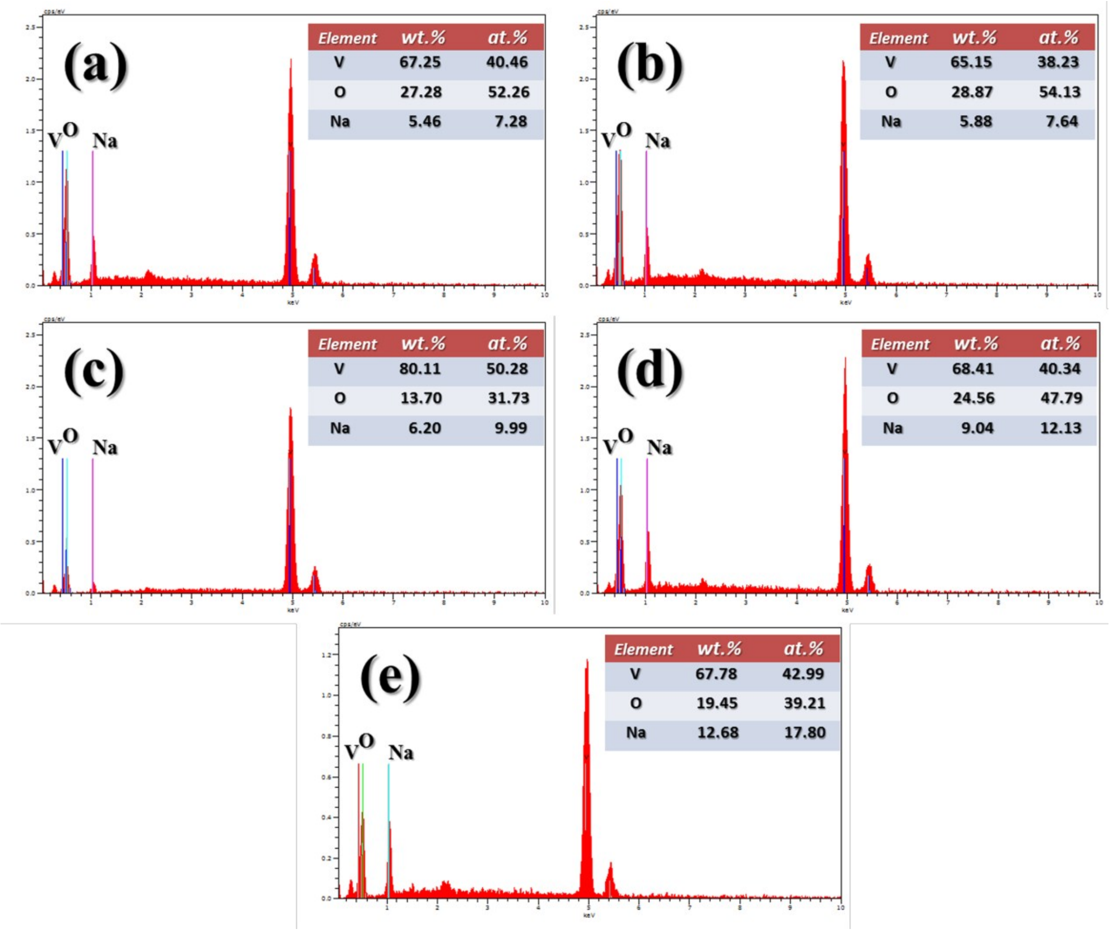

(a)

| Element | wt.% | at.% |
|---|---|---|
| V | 67.25 | 40.46 |
| O | 27.28 | 52.26 |
| Na | 5.46 | 7.28 |

(b)

| Element | wt.% | at.% |
|---|---|---|
| V | 65.15 | 38.23 |
| O | 28.87 | 54.13 |
| Na | 5.88 | 7.64 |

(c)

| Element | wt.% | at.% |
|---|---|---|
| V | 80.11 | 50.28 |
| O | 13.70 | 31.73 |
| Na | 6.20 | 9.99 |

(d)

| Element | wt.% | at.% |
|---|---|---|
| V | 68.41 | 40.34 |
| O | 24.56 | 47.79 |
| Na | 9.04 | 12.13 |

(e)

| Element | wt.% | at.% |
|---|---|---|
| V | 67.78 | 42.99 |
| O | 19.45 | 39.21 |
| Na | 12.68 | 17.80 |

**Figure S6.** Energy spectrums of samples prepared from two-step hydrothermal method. All samples were initially hydrothermally treated at 180 ºC for 48 hours in the first step, then further treated at 180 ºC for (a) 2 h, (b) 6 h, (c) 12 h, (d) 24 h, (e) 48 h during the second step.

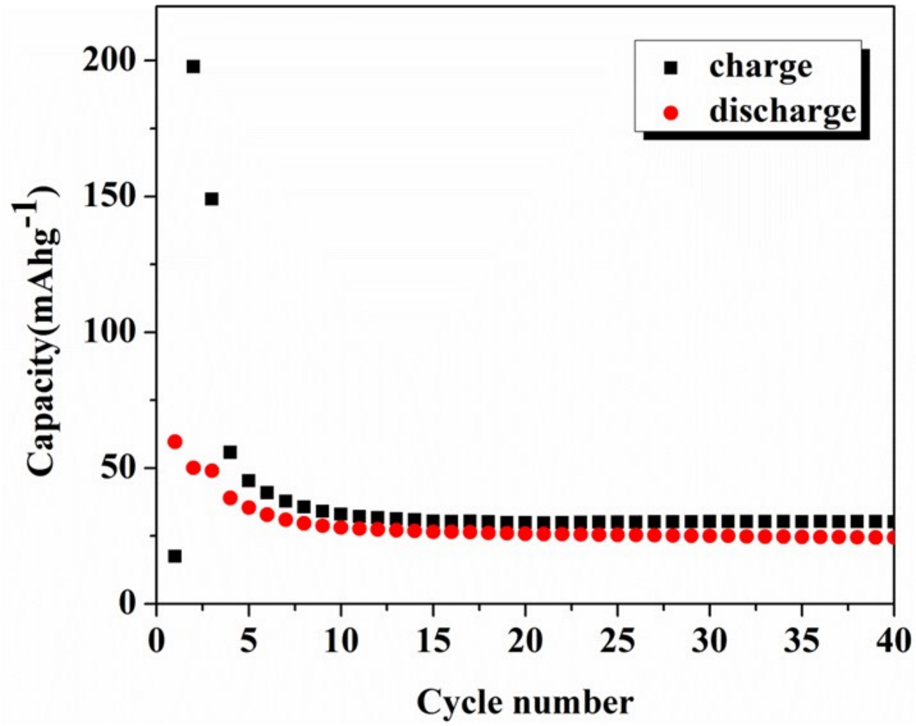

**Figure S7.** Cycling profile when the cell was firstly charged, and then discharged between at 20 mA/g current density.

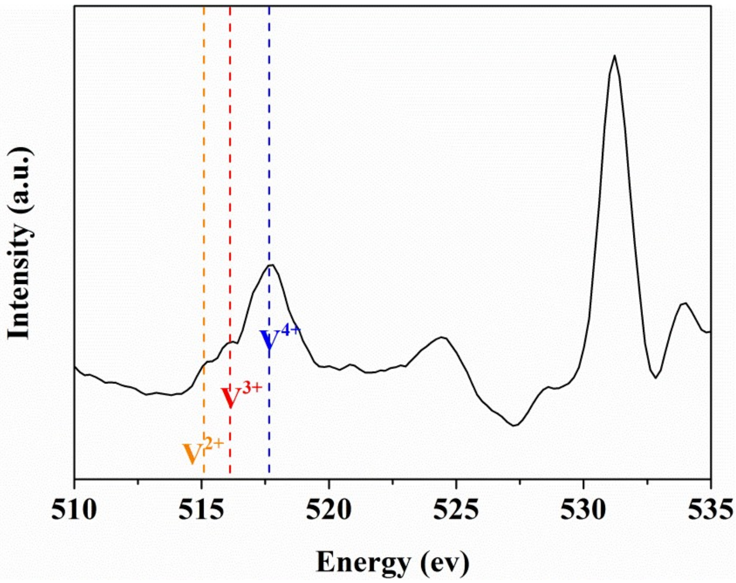

**Figure S8.** XANES for V *L*-edge absorption spectra through soft ray when the cell was discharged to 0.01 V in the first cycle.

## Discussion on XANES (Figure S8)

When the cell was discharged to 0.01 V in the first cycle, it was disassembled and the electrode materials were separated from current collector to conduct the corresponding XANES measurements. Some lower valence states of 2+, 3+ and 4+ for V can be found when $NaV_2O_5$ was discharged to 0.01 V.[5] It means that more and more Na-ions have been inserted to interlayers of $Na_xV_2O_5$ during discharging.

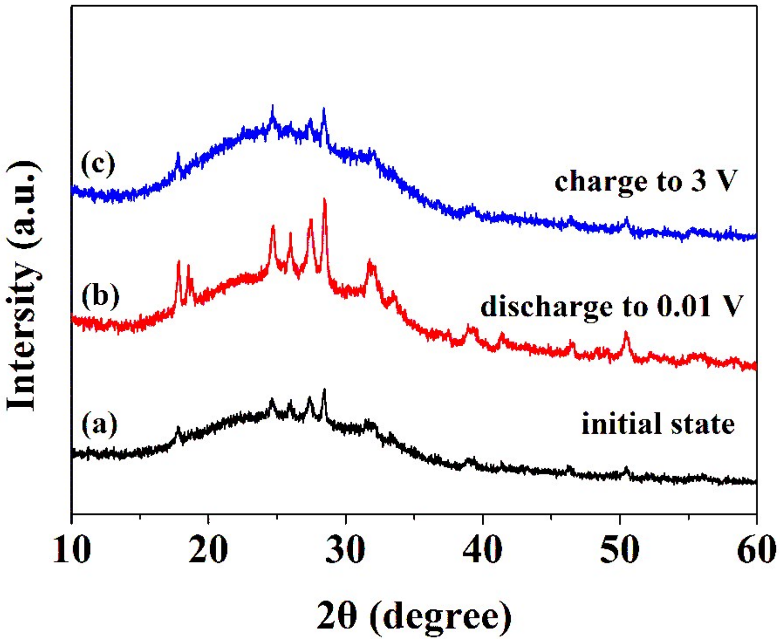

**Figure S9.** Ex-situ XRD patterns which are collected at different discharged and charged state in the first cycle. (a) Initial state of $NaV_2O_5$; (b) discharge to 0.01 V and the product become $Na_xV_2O_5$ (PDF card #24-1157, $P_{21mn}$, a=1.13 nm, b=0.36 nm, c=0.48 nm); (c) charge to 3 V and the product turns back to be $NaV_2O_5$. And, the ex-situ measurements were conducted by separating the electrode materials from the current collector.

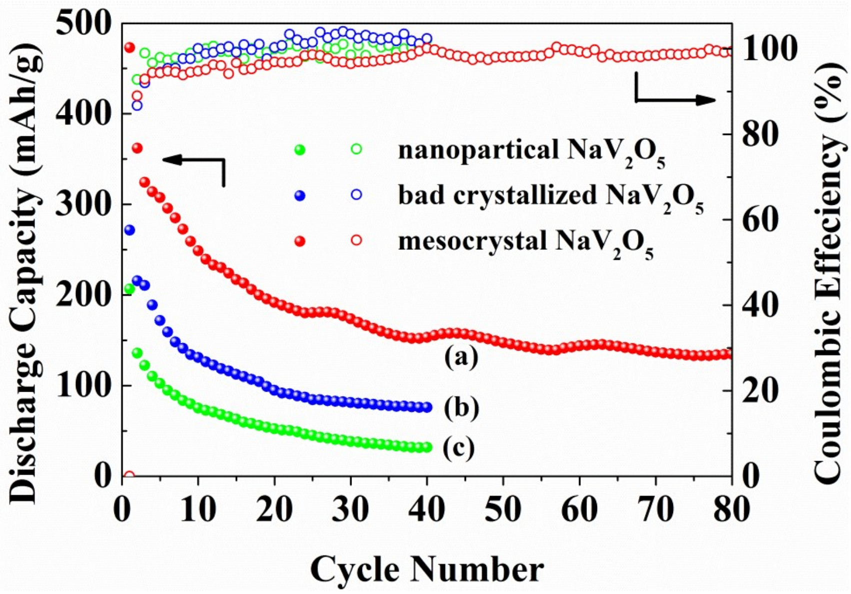

**Figure S10.** Cycling performance of different structured $NaV_2O_5$ at the current density of 150 mA/g. (a) Good crystalized mesocrystal $NaV_2O_5$ synthesized at 180 °C for the first step time of 48 h and the second one of 48 h under the two-step hydrothermal conditions; (b) bad crystalized $NaV_2O_5$ synthesized at 180 °C for the first step time of 38 h and the second one of 48 h under the two-step hydrothermal conditions; (c) non-mesocrystal $NaV_2O_5$ nanoparticals synthesized through solid-state method.

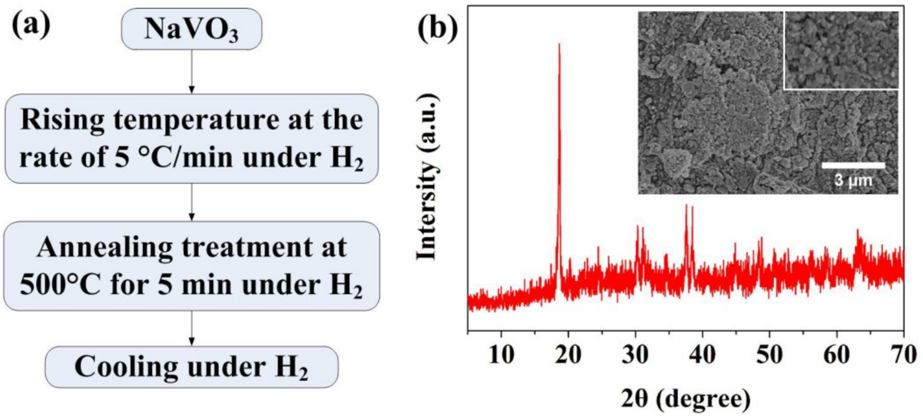

**Figure S11.** Synthesis of non-mesocrystal $NaV_2O_5$ nanoparticals. (a) Flow charts of solid-state synthesis; (b) XRD pattern (the inset is corresponding SEM image).

### Discussion on the synthesis of non-mesocrystal $NaV_2O_5$ nanopartical. (Figure S8)

Analytical grade $NaVO_3$ was received from Sinopharm Chemical Reagent Co., Ltd, China, and used without further purification. Appropriate amounts of $NaVO_3$ was put into the tube furnace, and then it was heated to 500 °C with a rising rate of 5 °C/min and kept for 5 min.[6-8] The whole synthesis process is under $H_2$ atmosphere (5% $H_2$/Ar). The XRD pattern shows that the as-synthesized product is $NaV_2O_5$ (Figure S11 (b)), and the SEM inset shows the morphology is non-mesocrystal nanoparticals.

**Table S1.** Detailed refined data of $NaV_2O_5$

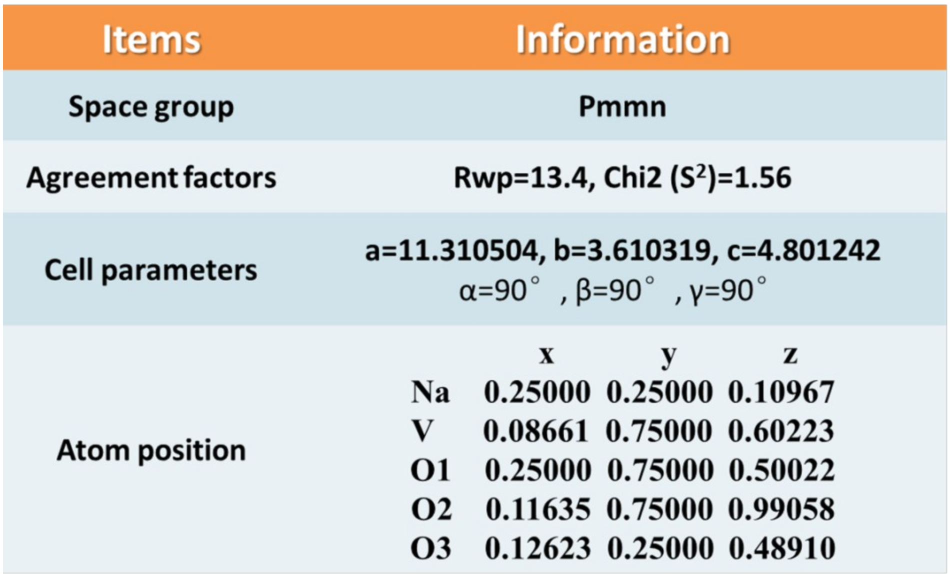

| Items | Information | | | |
|---|---|---|---|---|
| Space group | Pmmn | | | |
| Agreement factors | Rwp=13.4, Chi2 ($S^2$)=1.56 | | | |
| Cell parameters | a=11.310504, b=3.610319, c=4.801242<br>α=90° , β=90° , γ=90° | | | |
| Atom position | | x | y | z |
| | Na | 0.25000 | 0.25000 | 0.10967 |
| | V | 0.08661 | 0.75000 | 0.60223 |
| | O1 | 0.25000 | 0.75000 | 0.50022 |
| | O2 | 0.11635 | 0.75000 | 0.99058 |
| | O3 | 0.12623 | 0.25000 | 0.48910 |

**Table S2.** Observed Raman active modes of the $NaV_2O_5$ nanobelts.

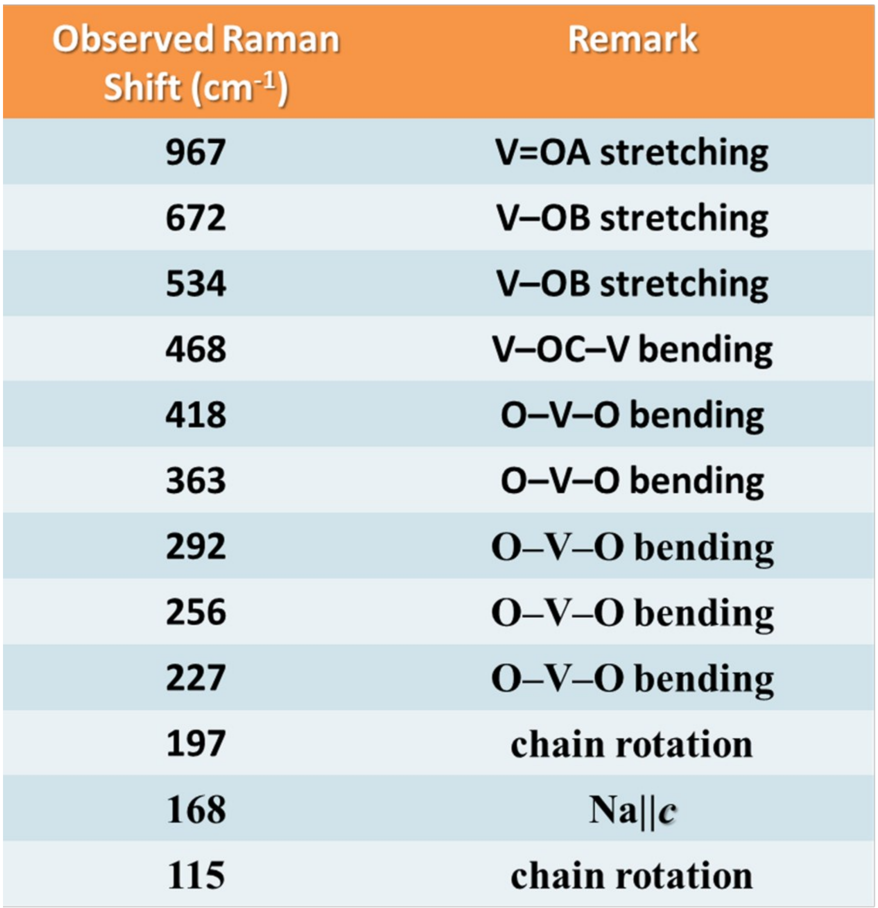

| Observed Raman Shift ($cm^{-1}$) | Remark |
|---|---|
| 967 | V=OA stretching |
| 672 | V–OB stretching |
| 534 | V–OB stretching |
| 468 | V–OC–V bending |
| 418 | O–V–O bending |
| 363 | O–V–O bending |
| 292 | O–V–O bending |
| 256 | O–V–O bending |
| 227 | O–V–O bending |
| 197 | chain rotation |
| 168 | Na\|\|*c* |
| 115 | chain rotation |

**Table S3.** Atom contents of Na-ions in the products for different treatment time under the two-step hydrothermal conditions.

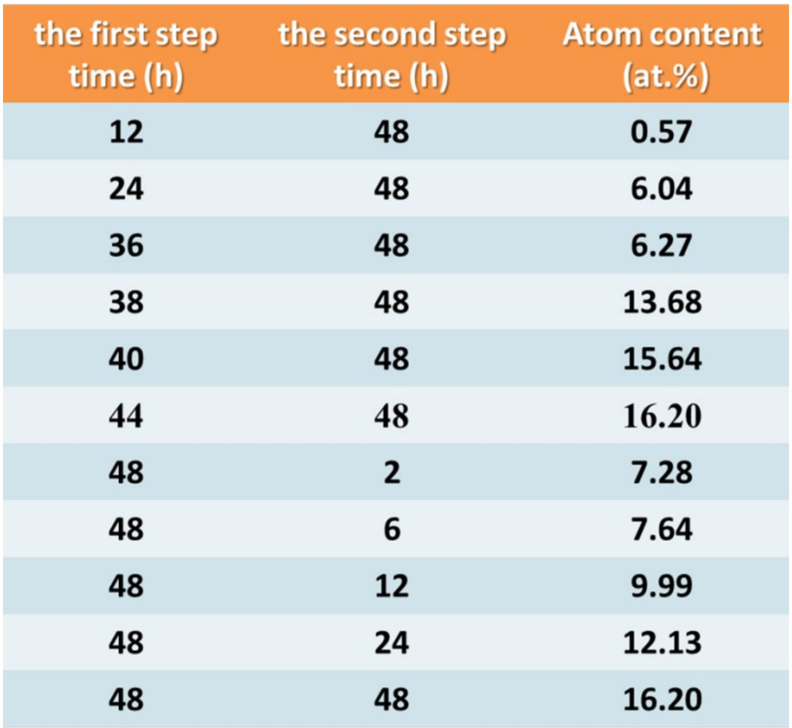

| the first step time (h) | the second step time (h) | Atom content (at.%) |
|---|---|---|
| 12 | 48 | 0.57 |
| 24 | 48 | 6.04 |
| 36 | 48 | 6.27 |
| 38 | 48 | 13.68 |
| 40 | 48 | 15.64 |
| 44 | 48 | 16.20 |
| 48 | 2 | 7.28 |
| 48 | 6 | 7.64 |
| 48 | 12 | 9.99 |
| 48 | 24 | 12.13 |
| 48 | 48 | 16.20 |

## Reference

1. N. Leopold and B. Lendl, *J. Phys. Chem. B*, 2003, **107**, 5723-5727.
2. D. G. Leaist, *Can. J. Chem.*, 1983, **61**, 1494-1499.
3. Y. Gao, S. Wang, H. Luo, L. Dai, C. Cao, Y. Liu, Z. Chen and M. Kanehira, *Energy Environ. Sci.,*, 2012, **5**, 6104-6110.
4. V. S. Reddy Channu, R. Holze, I.-H. Yeo, S.-i. Mho and R. Kalluru, *Appl. Phys. A*, 2011, **104**, 707-711.
5. G Cressey, C. M. B. Henderson and G. van der Laan, *Phys. Chem. Minerals*, 1993, **20**, 111-119.
6. A. I. Smirnov, M. N. Popova, A. B. Sushkov, S. A. Golubchik, D. I. Khomskii,

M. V. Mostovoy, A. N. Vasil'ev, M. Isobe and Y. Ueda, *Physical Review B*, 1999, **59**, 14546-14551.

7. A. I. Smirnov, S. S. Sosin, R. Calemczuk, V. Villar, C. Paulsen, M. Isobe and Y. Ueda, *Physical Review B*, 2000, **63**, 014412.

8. H. Smolinski, C. Gros, W. Weber, U. Peuchert, G. Roth, M. Weiden and C. Geibel, *Phys. Rev. Lett.*, 1998, **80**, 5164-5167.